

# Efficient Quasiparticle Determination beyond the Diagonal Approximation via Random Compression

Annabelle Canestraight\*

*Department of Chemical Engineering, University of California, Santa Barbara, CA 93106-9510, U.S.A.*

Xiaohe Lei

*Department of Chemistry and Biochemistry, University of California, Santa Barbara, CA 93106-9510, U.S.A.*

Khaled Z. Ibrahim

*Applied Mathematics and Computational Research Division,  
Lawrence Berkeley National Laboratory, Berkeley, CA 94720, USA*

Vojtěch Vlček

*Department of Chemistry and Biochemistry, University of California, Santa Barbara, CA 93106-9510, U.S.A. and  
Department of Materials, University of California, Santa Barbara, CA 93106-9510, U.S.A.*

(Dated: September 28, 2023)

Calculations of excited states in Green’s function formalism often invoke the diagonal approximation, in which the quasiparticle states are taken from a mean-field calculation. Here, we extend the stochastic approaches applied in the many-body perturbation theory and overcome this limitation for large systems in which we are interested in a small subset of states. We separate the problem into a core subspace, whose coupling to the remainder of the system environment is stochastically sampled. This method is exemplified on computing hole injection energies into CO<sub>2</sub> on an extended gold surface with nearly 3000 electrons. We find that in the extended system, the size of the problem can be compressed up to 95% using stochastic sampling. This result provides a way forward for self-consistent stochastic methods and determining Dyson orbitals in large systems.

*Introduction* Single particle states are frequently used in the study of excitation phenomena such as photoionization, electron injection, and generally optical transitions[1–9]. The physical interpretation of such single particle states often depends on the specific type of observables[7, 10]. In particular, Dyson orbitals, which correspond to the probability amplitude distribution of a specific electron or hole excitation (i.e., quasiparticle state), are directly accessible via orbital tomography and provide insights into the relation between energies and real-space distribution of single particle excitation[11, 12]. This has fundamental implications for chemistry – e.g., hybridization of quasiparticles on surfaces governs the propensity for direct injection of an electron [9]. These are just a few compelling reasons to account for the physically meaningful orbital distributions, especially for problems concerning (chemical) interfaces.

In practice, however, single-particle states for interfacial systems are typically taken from the Density Functional Theory (DFT) [13–15], as the cost of higher level theory is too high. While DFT can handle extremely large systems[16], these calculations can not, even in principle, yield quasiparticle (QP) energies or the Dyson orbitals[7, 17]. A natural and widely applied extension, especially in condensed matter problems, is application of the Many Body Perturbation Theory (MBPT) employing Green’s function formalism[7, 18–20]. In particular,

the *GW* approximation, which truncates the correlation expansion to non-local charge density fluctuations, has emerged as arguably the most popular approach[21, 22] and higher order corrections emerged recently[23–26]. Its self-consistent solution yields both QP energies and the Dyson orbitals [27–29]. However, it is common to apply *GW* approach as a one-shot correction,  $G_0W_0$ , employing the Kohn-Sham Green’s function  $G_0$  and the screened coulomb interaction  $W_0$  derived from the underlying Kohn Sham DFT solutions. Despite its approximate nature,  $G_0W_0$  often provides good estimates of band gaps[29–34]. The use of one-shot corrections has been largely motivated by the computational cost, which scales as  $\mathcal{O}(N^4)$  with the number of electrons in conventional implementations[35, 36]. The computational cost has been significantly decreased by stochastic sampling approaches in *GW* (and post-*GW*) to be nearly linear; 1000’s of states can thus be studied[37–41]. However, even in the stochastic *GW*, “updating” the single-particle basis (i.e., finding the Dyson orbitals) is difficult[42] and, in practice, usually avoided[43]. Routine calculations of QP orbitals in realistic systems with thousands of electrons are still elusive. This is true even if one is, in principle, interested in treating a *small subset* of states, as exemplified in this work (see below).

Here, we tackle this problem and present a scheme without the diagonal approximation for realistic nanoscale systems. This stochastic framework is exemplified for CO<sub>2</sub> molecule on a large Au slab. For this problem, the surface contributions to the orbitals are sampled, drastically reducing the cost of QP calculations. This

\* acanestraight@ucsb.edu

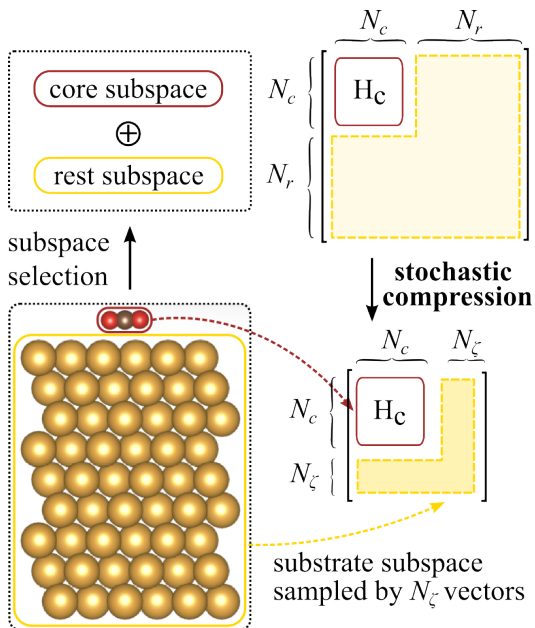


FIG. 1. Illustration of the stochastic compression technique, which samples the “rest subspace” using a set of (filtered) random vectors, here spanning the single particle states of the gold substrate.

method divides the system into a set of states in an “core” subspace, treated by standard stochastic MBPT, and a rest space, for which additional sampling is introduced. This step is combined with a search over the fixed-point solutions of the frequency-dependent QP Hamiltonian, which is basis representation independent and thus enables the use of random vectors.

We apply these methods to a prototypical system of a small molecule on a plasmonic surface ( $\text{CO}_2$  on Au illustrated in the inset in Fig. 1). In the practical demonstration for an extended Au (111) surface with 270 atoms (2986 electrons), we found convergence in the hybridized HOMO energy with a 95% rank compression compared to evaluation in the full canonical orbital basis. This success provides a way to use costly high-level theories to study realistic chemical systems.

*Formalism* The time-ordered Green’s function (GF) contains information about the quasiparticle (QP) energy spectrum and lifetimes, and it corresponds to the probability amplitude of a QP propagation between two space-time points  $\mathbf{r}, t$  and  $\mathbf{r}', t'$ . In the Lehmann representation, it is expressed as

$$G(\mathbf{r}, \mathbf{r}', \omega) = \sum_n \left[ \frac{\psi_n(\mathbf{r})\psi_n(\mathbf{r}')^*}{\omega - \varepsilon_n - i\eta} \right], \quad (1)$$

where the Dyson orbitals are obtained as  $\psi_n(\mathbf{r}) = \langle \Psi_{N-1}^n | \hat{\psi}(\mathbf{r}) | \Psi_N^0 \rangle$  from the  $N$ -particle ground state and the  $n^{\text{th}}$  excited state of the  $N - 1$  particle system, where  $\hat{\psi}(\mathbf{r})$  is the field operator. The poles of the GF are located at the QP energies,  $\varepsilon_n$ , here corresponding to the

charge removal [7]. Charge addition is treated analogously. The GF poles are conveniently expressed as solutions to a non-linear eigenvalue problem for an effective Hamiltonian obtained by downfolding interactions with the system[7]:

$$\hat{H}_{QP}(\omega) |\psi\rangle = \omega |\psi\rangle \quad (2)$$

In practice, the QP Hamiltonian is divided into a static and local term,  $H_0$ , which typically contains all one-body contributions, while a space-time non-local portion is represented by the self-energy operator  $\tilde{\Sigma}$ [22]. The latter is approximated by selected types of interaction diagrams (and their resummation). As  $\tilde{\Sigma}$  is conceptually equivalent to the exchange-correlation potential applied in the Kohn-Sham density functional theory (KS DFT), the QP Hamiltonian is practically constructed as a perturbative correction on top of such a mean-field starting point:

$$\hat{H}_{QP}(\omega) = \hat{H}_{0,\text{KS}} - \hat{V}_{xc} + \hat{\Sigma}(\omega), \quad (3)$$

where  $\hat{H}_{0,\text{KS}}$  is the KS DFT Hamiltonian.

Further, the “one-shot” correction corresponds to:

$$\Sigma(\mathbf{r}, \mathbf{r}', \omega) = i \int \frac{d\omega'}{2\pi} G_0(\mathbf{r}, \mathbf{r}', \omega + \omega') W_0(\mathbf{r}, \mathbf{r}', \omega'), \quad (4)$$

where  $G_0$  has poles at the DFT Kohn Sham eigenvalues,  $\varepsilon_0$ , and  $W_0$  is the screened coulomb interaction. The self-consistency requires repeated construction of  $\Sigma$  and re-evaluation of Eq. 2; multiple flavors of self-consistent approaches have been developed [27, 28]. Typically, the convergence pattern is smooth. If the KS DFT single-particle states are close to the Dyson orbitals, the “one-shot” correction provides good estimates of QP energies, yet the quality of the mean-filed eigenstates are not *a priori* known.

A step beyond this practice is to diagonalize  $H_{QP}$  in Eq. 2 in the orbital basis, yielding Dyson orbitals (in the first iteration) and updated one-shot QP energies in the *GW* approximation[7]. Note that, in principle, the nonlinear problem in Eq. 2 holds for multiple values of  $\omega$  associated with satellite features [23, 44, 45]. In this work, we will focus only on the primary QP peaks, i.e., we seek a single solution to the QP Hamiltonian in the vicinity of  $\varepsilon_0$  and look for the fixed point solutions to  $\omega_i = \langle \phi_i | \hat{H}_{QP}[\omega_i] | \phi_i \rangle$ . Note that  $H_{QP}$  is non-hermitian, and each QP state, in general, corresponds to  $H_{QP}$  computed at a different frequency.

In practical schemes[29, 43, 46, 47], it is common to construct a single “static” effective Hamiltonian (yielding orthogonal eigenstates). However, due to the non-linearity of this problem, it is not entirely clear at what frequency the self-energy should be evaluated. For strongly diagonally dominant  $H_{QP}$ , i.e., those where KS DFT orbitals are, in fact, close to the Dyson orbitals, one may evaluate  $\omega_i$  as the fixed point solution for the diagonal entries. The remaining off-diagonal self-energy is e.g.,  $\Sigma_{ij} = \frac{1}{4} [\Sigma_{ij}(\omega_i) + \Sigma_{ji}(\omega_i) + \Sigma_{ij}(\omega_j) + \Sigma_{ji}(\omega_j)]$ . In this

form, it is possible to construct a static and hermitized QP Hamiltonian. By enforcing the hermicity of  $H_{QP}$ , we impose that the resulting QP states are orthonormal. The QP energies are purely real, corresponding to an infinite lifetime QP. Alternatively, one can therefore relax the latter step by taking  $\Sigma_{ij} = \frac{1}{2} [\Sigma_{ij}(\omega_i) + \Sigma_{ij}(\omega_j)]$ .

Note that both approaches strongly depend on the basis choice. We illustrate this in detail in the Supporting Information (SI) for the acrolein molecule, for which the magnitudes of the off-diagonal terms are 98.5% smaller than the diagonal ones for the canonical KS DFT basis. The situation changes dramatically when localized (unitary transformed) orbitals are employed. Hence, depending on the construction of a single  $H_{QP}$ , the resulting QP energies change by as much as 10% and translate to changes of 0.77 eV on average for acrolein.

Since our goal is to determine Dyson orbitals for a selected subspace of interest (which will be constructed from localized basis states), we avoid any approximation to the fixed point solution. In this method, the whole QP Hamiltonian is evaluated at multiple frequencies, and the QP eigenvalues are found as the fixed point solutions to Eq. 2. No assumptions are further made about the hermicity of the Hamiltonian matrix; a graphical example of such a fixed point solution for the  $H_{QP}$  is also illustrated in the SI.

*Stochastic Compression of QP states* When studying a large system with a subspace of particular interest, it is prohibitively expensive to employ all  $M$  electronic states. It is also insufficient to assume that the Hamiltonian matrix takes a block-diagonal form due to the coupling between the subspace and its orthogonal complement. To handle such a case, we propose a method of stochastic matrix compression where a portion of the  $H_{QP}$  matrix is represented by a set of random vectors. These vectors sample a large portion of the Hilbert space, which overall contributes to the QP shift and affects the Dyson orbitals, but for which each individual single particle state has only a limited contribution.

As illustrated in Fig. 1, we separate the “core subspace” spanned by  $N_c$  deterministic states,  $\{\phi^c\}$ , (e.g., the original KS DFT eigenstates), and the remainder spanned by a  $N_s$  stochastic states  $\{\zeta\}$ , constructed as a random linear combination of the KS states that are orthogonal to the  $\{\phi^c\}$  set:  $|\zeta\rangle = \sum_{i=1}^{N_s} c_i |\phi_i\rangle$ . In the final step, the individual random states are orthogonalized via the Gram-Schmidt process. Because this change of basis is guaranteed to be a unitary transformation of the Hamiltonian matrix, when the whole system is diagonalized, the resulting eigenstates will be the same. When the Hamiltonian matrix is truncated in this new stochastic basis, the coupling of each stochastic state to the core subspace will represent the subspace interaction with the full environment. In this way, we have “compressed” the information of the whole system environment into a single state. Given that the fixed point solution is basis independent (as illustrated in Fig. S.3), a total number of states  $N_c + N_s$  is the same as the dimension of

$H_{QP}$ ,  $M$ , we necessarily obtain the same QP energies. For fewer random states,  $N_c + N_s < M$ , and the computation is less expensive. Note that the QP energy has a finite statistical error, which decreases as  $1/\sqrt{N_s}$  with the number of states sampling the off-diagonal self-energy contributions. As we show below, the convergence of the QP energies is smooth. Further, note that instead of the canonical single particle states in the above equation, we achieve further speedup if already preselected (filtered) subset of states (orthogonal to the  $\{\phi^c\}$ ) are used in the construction of  $|\zeta\rangle$ .

*Results* We now demonstrate the method practically for the CO<sub>2</sub> molecule on the Au substrate for which we intend to extract the energies of quasi-hole states on the molecule (i.e., corresponding to the charge removal energies from CO<sub>2</sub> on the surface). We first construct a minimal example on which we can solve entirely and illustrate how stochastic sampling smoothes the convergence of the QP energies. Later, we show a realistic example with nearly 3,000 electrons, which cannot be easily solved without the sampling methodology.

We will demonstrate the success of our stochastic sampling method on a minimal system of CO<sub>2</sub> on a bilayer of 8 gold atoms. This system contains only 52 occupied states, which we also treat explicitly. Note that, in principle, the hybridization extends beyond merely the occupied manifold, but to illustrate the methodology, we consider only the rotation within the occupied subspace. To see the surface-induced changes, calculate the QP states for a CO<sub>2</sub> molecule in a vacuum ( $N = 8$ ) and for the minimal composite system ( $N = 52$ ). We find that the seven lowest valence states of the molecule shift in energy when the substrate is included, but the eigenvectors (orbitals) do not change in response to the gold substrate.

In contrast, HOMO state behaves differently: no single state would correspond to the molecular HOMO (either the canonical DFT or Dyson orbitals computed at the  $G_0W_0$  level). Instead, there are multiple *hybridized* states sufficiently localized on the molecule, whose eigenvalues lay within a small range of energies. We aim to characterize them and, consequently, to find a characteristic QP energy for this distribution of HOMO QP for the CO<sub>2</sub> molecule on Au.

We thus define a “core subspace” comprising the states with the most molecular character. In practice, they are identified based on projection onto localized (unitary transformed) orbitals centered on CO<sub>2</sub>, e.g., using the molecular reconstruction technique which is applied here[41, 48]. The corresponding projection value is:

$$P_i = \sum_j |\langle \xi_j | \phi_i \rangle|^2 \quad (5)$$

Here,  $\{|\xi\rangle\}$  and  $\{|\phi\rangle\}$  are the sets of transformed (localized) and canonical KS DFT states respectively. Each KS state with  $P$  greater than a chosen threshold is included in the core region. This preselection separates the “core” subspace from the rest.

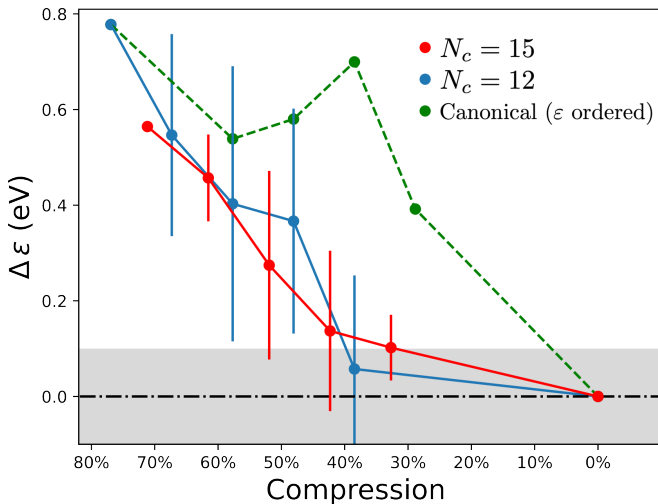


FIG. 2. **Hybridized HOMO Convergence (Minimal System)**: Core sizes of  $N_c = 12$  and  $N_c = 15$  are used, with the remaining states sampled with equal weight. In contrast, the adding the states by energy ( $\epsilon$  ordered) demonstrates the lack of smooth convergence. The gray-shaded region shows where the spectrum converges within 0.1 eV

We now track the fixed point HOMO QP solution with the number of states considered in the  $H_{QP}$ , i.e., we gradually add more states outside of the core subspace. The molecular HOMO is hybridized with many of the surface states. We thus define a single energy for this state by taking its mean value, constructed by weighting by the projection onto the HOMO of  $\text{CO}_2$  in a vacuum. The results are shown by the green color in Fig. 2. The left-most point represents only the core space, containing 12 orbitals corresponding to 23% of the entire  $H_{QP}$ . The size of the problem is increased by adding states depending on their distance from the KS DFT HOMO energy, as one would expect that the hybridization of states will be small for energetically distant states. This does not produce a smooth convergence (green line in Fig. 2) as some surface hybridization is due to Au orbitals that are far from the core subspace.

To demonstrate the stochastic approach, we now instead sample the remaining KS states using random vectors:

$$|\zeta\rangle = \frac{1}{\sqrt{N_e}} \sum_{j=1}^{N_e} w_j e^{i\theta_j} |\phi_j\rangle \quad (6)$$

Here  $\theta_j \in [0, 2\pi]$  is randomly chosen, and  $N_e$  is the number of “rest” states used with weight  $w_i$ . Note that we can either sample all remaining states evenly ( $w_i = 1/\forall i$ ), but generally, we consider a random selection from a distribution within the sampled subspace (determined by  $P_i$  in Eq. 5) as we show later.

Once we have obtained the set  $\{\zeta\}$ , we randomly draw  $N_s$  of them and the fixed point solution is then found for  $H_{QP}$  with the dimension of  $N_c + N_s$ . The results for

$N_c = 12$  and variable  $N_s$  is in Fig. 2 and shows a monotonic and smooth convergence towards to the asymptotic value (obtained for the entire 52 occupied states). The stochastic sampling was repeated ten times for each step with a different set of  $N_s$  random vectors; the standard deviations are indicated in the plot and they naturally disappear in the complete basis limit. For instance, for  $N_s = 20$ , i.e., 62% of the entire system, we see a difference of  $0.057 \pm 0.19$  eV between the mean HOMO QP energies. For an increased core space,  $N_c = 15$ , we see that the HOMO QP value converges similarly, i.e., the size of the core space is not changing the convergence profile significantly. For  $N_s = 20$  (i.e., 32.5% compression of matrix rank), the resulting spectrum mean falls within a 100 meV from the value obtained from the diagonalization of the full matrix.

Without any prior knowledge or arbitrary truncation of the KS states, we can capture molecule-surface hybridization effects by employing stochastic states representing the substrate environment. This description is systematically improvable by increasing both  $N_c$  and  $N_s$ . In general, the cost reduction provided by the stochastic sampling is due to circumventing the summation over many states that contribute either similarly or very little to the expectation values in question[49]. For a small system such as the one used here, the amount of compression is less significant as most of the states contribute to the QP HOMO energy.

We now turn to a realistic large-scale system for which such a calculation would not be possible with standard methods. Here, we study  $\text{CO}_2$  molecule on an extended Au-111 surface of 270 atoms, containing 2986 electrons. The system is treated analogously to the minimal example: we selected a core subspace of 15 and 25 states. Due to the molecule-surface hybridization,  $N_c = 15$  is the minimal size of the core space identified for this particular problem. Next, the stochastic sampling uses a filtered distribution in Eq. 6 in which we consider a linear combination of states that are sufficiently localized on the molecules. In practice, this step determines the sampled subspace, which is practically restricted to states with  $P$  greater than a selected threshold,  $P_T$ . Here we consider two cases  $P_T = 10^{-3}$  and  $P_T = 5 \times 10^{-4}$ .

From Fig. 3 we can see that the HOMO energy converges with only 5% of the total number of states used[50]. For slightly increased selectivity (i.e., lower projection threshold  $P$ ), the stochastic sampling of the hybridization converges similarly. Further, the size of the core subspace does not significantly impact the convergence rate: when  $N_c = 25$  with the filtering threshold of  $P_T = 5 \times 10^{-4}$ , the curve matches that of the  $N_c = 15$  for the same value of  $P_T$ . This suggests that the size of the core subspace can be decreased, possibly at the expense of using more stochastic samplings.

Finally, note that when the orbital re-hybridization is used at the  $G_0W_0$  level, the HOMO QP energy moves down in energy by more than 1 eV. Since approximate semilocal KS DFT is known to suffer from overdelocaliza-

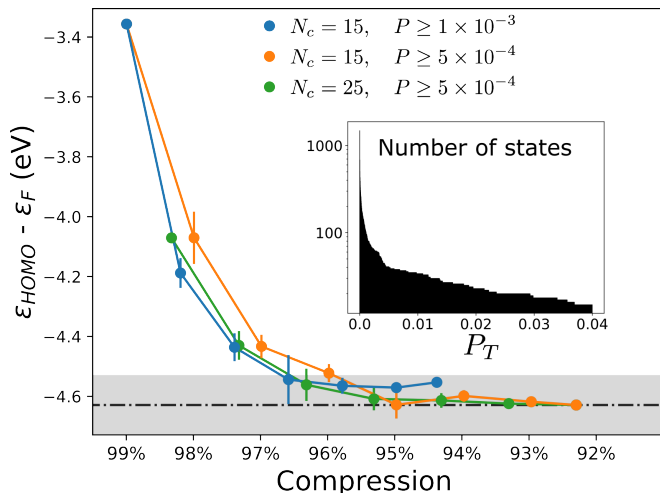


FIG. 3. **Hybridized HOMO Convergence (Large System with 2986 electrons):** Convergence is demonstrated across multiple core sizes and stochastic sampling filterings. The shaded region indicates that the HOMO is within 0.1 eV of the converged value. The inset shows the log-scale histogram of the number of states for which the projection value  $P \geq P_T$ , where  $P_T$  is the filtering cutoff (see text).

tion, it is expected that the physical Dyson orbitals are more localized than the canonical KS DFT eigenstates. In turn, stronger localization of HOMO is typically associated with its energy decrease[9]. These observations are thus in line with what the MBPT should accomplish and underline the need for more appropriate treatment of surface phenomena.

*Outlook* The rapid convergence of the QP energies with  $N_s$  implies that when we stochastically sample the

matrix, aided by preselection and filtering, we can represent the full QP spectrum for a molecule that hybridizes with an extended surface using less than 5% of the system. The  $H_{QP}$  matrix size is thus compressed by 95%. This is largely due to the significant “redundancy” of information encoded in individual single-particle states, and the sampling allows sampling all (or a large filtered portion of them) simultaneously through random vectors. The approach presented here will enable the treatment of large-scale interfacial problems and opens the door for efficient self-consistent stochastic MBPT.

## ACKNOWLEDGEMENTS

The development (A.C., X.L., and V.V.) of the stochastic compression technique was supported by the NSF CAREER award (DMR-1945098). The implementation and numerical testing (A.C., K.I., and V.V.) is based upon work supported by the U.S. Department of Energy, Office of Science, Office of Advanced Scientific Computing Research and Office of Basic Energy Sciences, Scientific Discovery through Advanced Computing (SciDAC) program under Award Number DE-SC0022198. This research used resources of the National Energy Research Scientific Computing Center, a DOE Office of Science User Facility supported by the Office of Science of the U.S. Department of Energy under Contract No. DE-AC02-05CH11231 using NERSC award BES-ERCAP0020089.

- 
- [1] Maxim V. Ivanov, Felix H. Bangerter, and Anna I. Krylov. Towards a rational design of laser-coolable molecules: insights from equation-of-motion coupled-cluster calculations. *Phys. Chem. Chem. Phys.*, 21:19447–19457, 2019.
  - [2] Maxim V. Ivanov, Thomas-C. Jagau, Guo-Zhu Zhu, Eric R. Hudson, and Anna I. Krylov. In search of molecular ions for optical cycling: a difficult road. *Phys. Chem. Chem. Phys.*, 22:17075–17090, 2020.
  - [3] Samer Gozem, Robert Seidel, Uwe Hergenbahn, Evgeny Lugovoy, Bernd Abel, Bernd Winter, Anna I. Krylov, and Stephen E. Bradforth. Probing the electronic structure of bulk water at the molecular length scale with angle-resolved photoelectron spectroscopy. *The Journal of Physical Chemistry Letters*, 11(13):5162–5170, 2020. PMID: 32479725.
  - [4] Peter Puschnig, Stephen Berkebile, Alexander J. Fleming, Georg Koller, Konstantin Emtsev, Thomas Seyller, John D. Riley, Claudia Ambrosch-Draxl, Falko P. Netzer, and Michael G. Ramsey. Reconstruction of molecular orbital densities from photoemission data. *Science*, 326(5953):702–706, 2009.
  - [5] Sergei Tretiak and Shaul Mukamel. Density matrix analysis and simulation of electronic excitations in conjugated and aggregated molecules. *Chemical Reviews*, 102(9):3171–3212, 2002. PMID: 12222985.
  - [6] Daniel Lüftner, Thomas Ules, Eva Maria Reinisch, Georg Koller, Serguei Soubatch, F Stefan Tautz, Michael G Ramsey, and Peter Puschnig. Imaging the wave functions of adsorbed molecules. *Proc. Natl. Acad. Sci. U. S. A.*, 111(2):605–610, January 2014.
  - [7] Richard M. Martin, Lucia Reining, and David M. Ceperley. *Interacting Electrons: Theory and Computational Approaches*. Cambridge University Press, 2016.
  - [8] Giovanni Onida, Lucia Reining, and Angel Rubio. Electronic excitations: density-functional versus many-body green’s-function approaches. *Rev. Mod. Phys.*, 74:601–659, Jun 2002.
  - [9] Xiaohu Lei, Annabelle Canestraight, and Vojtech Vlecek. Exceptional spatial variation of charge injection energies on plasmonic surfaces. *The Journal of Physical Chemistry Letters*, 0(0):8470–8476, 0. PMID: 37721434.
  - [10] Anna I. Krylov. From orbitals to observables and back. *The Journal of Chemical Physics*, 153(8):080901, 08

- 2020.
- [11] P. Puschnig, A. D. Boese, M. Willenbockel, M. Meyer, D. Lüftner, E. M. Reinisch, T. Ules, G. Koller, S. Soubatch, M. G. Ramsey, and F. S. Tautz. Energy ordering of molecular orbitals. *The Journal of Physical Chemistry Letters*, 8(1):208–213, 2017. PMID: 27935313.
- [12] Richard L. Martin. Natural transition orbitals. *The Journal of Chemical Physics*, 118(11):4775–4777, 02 2003.
- [13] Zhi-Zheng Wu, Xiao-Long Zhang, Zhuang-Zhuang Niu, Fei-Yue Gao, Peng-Peng Yang, Li-Ping Chi, Lei Shi, Wen-Sen Wei, Ren Liu, Zhi Chen, et al. Identification of cu (100)/cu (111) interfaces as superior active sites for co dimerization during co<sub>2</sub> electroreduction. *Journal of the American Chemical Society*, 144(1):259–269, 2021.
- [14] Ariel Biller, Isaac Tamblyn, Jeffrey B Neaton, and Leor Kronik. Electronic level alignment at a metal-molecule interface from a short-range hybrid functional. *The Journal of chemical physics*, 135(16):164706, 2011.
- [15] David A Egger, Zhen-Fei Liu, Jeffrey B Neaton, and Leor Kronik. Reliable energy level alignment at physisorbed molecule–metal interfaces from density functional theory. *Nano letters*, 15(4):2448–2455, 2015.
- [16] Joost VandeVondele, Urban Borštnik, and Jürg Hutter. Linear scaling self-consistent field calculations with millions of atoms in the condensed phase. *Journal of Chemical Theory and Computation*, 8(10):3565–3573, 2012. PMID: 26593003.
- [17] E. Engel and R.M. Dreizler. *Density Functional Theory: An Advanced Course*. Theoretical and Mathematical Physics. Springer Berlin Heidelberg, 2011.
- [18] Lars Hedin. New method for calculating the one-particle green’s function with application to the electron-gas problem. *Physical Review*, 139(3A):A796, 1965.
- [19] Mark S. Hybertsen and Steven G. Louie. First-principles theory of quasiparticles: Calculation of band gaps in semiconductors and insulators. *Phys. Rev. Lett.*, 55:1418–1421, Sep 1985.
- [20] R. W. Godby, M. Schlüter, and L. J. Sham. Self-energy operators and exchange-correlation potentials in semiconductors. *Phys. Rev. B*, 37:10159–10175, Jun 1988.
- [21] Giovanni Onida, Lucia Reining, and Angel Rubio. Electronic excitations: density-functional versus many-body green’s-function approaches. *Rev. Mod. Phys.*, 74:601–659, Jun 2002.
- [22] Dorothea Golze, Marc Dvorak, and Patrick Rinke. The GW compendium: A practical guide to theoretical photoemission spectroscopy. *Front. Chem.*, 7:377, July 2019.
- [23] Carlos Mejuto-Zaera, Guorong Weng, Mariya Romanova, Stephen J. Cotton, K. Birgitta Whaley, Norm M. Tubman, and Vojtěch Vlček. Are multi-quasiparticle interactions important in molecular ionization? *The Journal of Chemical Physics*, 154(12):121101, 2021.
- [24] Carlos Mejuto-Zaera and Vojtěch Vlček. Self-consistency in  $g\Gamma$  formalism leading to quasiparticle-quasiparticle couplings. *Phys. Rev. B*, 106:165129, Oct 2022.
- [25] Vojtěch Vlček. Stochastic vertex corrections: Linear scaling methods for accurate quasiparticle energies. *Journal of Chemical Theory and Computation*, 15(11):6254–6266, 2019. PMID: 31557012.
- [26] Guorong Weng, Rushil Mallarapu, and Vojtěch Vlček. Embedding vertex corrections in GW self-energy: Theory, implementation, and outlook. *The Journal of Chemical Physics*, 158(14):144105, 04 2023.
- [27] Alexander A Rusakov and Dominika Zgid. Self-consistent second-order green’s function perturbation theory for periodic systems. *The Journal of chemical physics*, 144(5), 2016.
- [28] Fabio Caruso, Patrick Rinke, Xinguo Ren, Angel Rubio, and Matthias Scheffler. Self-consistent gw: All-electron implementation with localized basis functions. *Physical Review B*, 88(7):075105, 2013.
- [29] F. Kaplan, F. Weigend, F. Evers, and M. J. van Setten. Off-diagonal self-energy terms and partially self-consistency in gw calculations for single molecules: Efficient implementation and quantitative effects on ionization potentials. *Journal of Chemical Theory and Computation*, 11(11):5152–5160, 2015. PMID: 26574312.
- [30] Jiachen Li, Ye Jin, Patrick Rinke, Weitao Yang, and Dorothea Golze. Benchmark of gw methods for core-level binding energies. *Journal of Chemical Theory and Computation*, 18(12):7570–7585, 2022. PMID: 36322136.
- [31] Vojtěch Vlček, Eran Rabani, Daniel Neuhauser, and Roi Baer. Stochastic gw calculations for molecules. *Journal of Chemical Theory and Computation*, 13(10):4997–5003, 2017. PMID: 28876912.
- [32] G-M Rignanese, X Blase, and SG Louie. Quasiparticle effects on tunneling currents: A study of c 2 h 4 adsorbed on the si (001)-(2× 1) surface. *Physical review letters*, 86(10):2110, 2001.
- [33] Michael Rohlfing, Peter Krüger, and Johannes Pollmann. Quasiparticle band-structure calculations for c, si, ge, gaas, and sic using gaussian-orbital basis sets. *Phys. Rev. B*, 48:17791–17805, Dec 1993.
- [34] Eric L. Shirley and Richard M. Martin. Gw quasiparticle calculations in atoms. *Phys. Rev. B*, 47:15404–15412, Jun 1993.
- [35] T Anh Pham, Huy-Viet Nguyen, Dario Rocca, and Giulia Galli. G w calculations using the spectral decomposition of the dielectric matrix: Verification, validation, and comparison of methods. *Physical Review B*, 87(15):155148, 2013.
- [36] Marco Govoni and Giulia Galli. Large scale gw calculations. *Journal of Chemical Theory and Computation*, 11(6):2680–2696, 2015. PMID: 26575564.
- [37] Vojtěch Vlček, Wenfei Li, Roi Baer, Eran Rabani, and Daniel Neuhauser. Swift g w beyond 10,000 electrons using sparse stochastic compression. *Physical Review B*, 98(7):075107, 2018.
- [38] Vojtěch Vlček, Eran Rabani, Daniel Neuhauser, and Roi Baer. Stochastic gw calculations for molecules. *Journal of Chemical Theory and Computation*, 13(10):4997–5003, 2017. PMID: 28876912.
- [39] Guorong Weng and Vojtěch Vlček. Quasiparticles and band structures in organized nanostructures of donor–acceptor copolymers. *The Journal of Physical Chemistry Letters*, 11(17):7177–7183, 2020. PMID: 32787318.
- [40] Mariya Romanova and Vojtěch Vlček. Decomposition and embedding in the stochastic gw self-energy. *The Journal of Chemical Physics*, 153(13), 2020.
- [41] Guorong Weng and Vojtěch Vlček. Efficient treatment of molecular excitations in the liquid phase environment via stochastic many-body theory. *The Journal of Chemical Physics*, 155(5):054104, 2021.
- [42] Mariya Romanova and Vojtěch Vlček. Stochastic many-body calculations of moiré states in twisted bilayer graphene at high pressures. *npj Computational Mate-*

- rials*, 8(1):11, Jan 2022.
- [43] Vojtěch Vlček, Roi Baer, Eran Rabani, and Daniel Neuhauser. Simple eigenvalue-self-consistent  $\bar{\Delta}GW$ . *The Journal of Chemical Physics*, 149(17):174107, 11 2018.
- [44] F. Aryasetiawan, L. Hedin, and K. Karlsson. Multiple plasmon satellites in na and al spectral functions from ab initio cumulant expansion. *Phys. Rev. Lett.*, 77:2268–2271, Sep 1996.
- [45] Johannes Lischner, G. K. Pálsson, Derek Vigil-Fowler, S. Nemsak, J. Avila, M. C. Asensio, C. S. Fadley, and Steven G. Louie. Satellite band structure in silicon caused by electron-plasmon coupling. *Phys. Rev. B*, 91:205113, May 2015.
- [46] M. Van Schilfgaarde, Takao Kotani, and S. Faleev. Quasiparticle self-consistent *gw* theory. *Phys. Rev. Lett.*, 96:226402, Jun 2006.
- [47] Takao Kotani, Mark van Schilfgaarde, and Sergey V. Faleev. Quasiparticle self-consistent *gw* method: A basis for the independent-particle approximation. *Phys. Rev. B*, 76:165106, Oct 2007.
- [48] Guorong Weng, Mariya Romanova, Arsineh Apelian, Hanbin Song, and Vojtěch Vlček. Reduced scaling of optimal regional orbital localization via sequential exhaustion of the single-particle space. *Journal of Chemical Theory and Computation*, 18(8):4960–4972, 2022. PMID: 35817013.
- [49] Roi Baer, Daniel Neuhauser, and Eran Rabani. Stochastic vector techniques in ground-state electronic structure. *Annual Review of Physical Chemistry*, 73(1):255–272, 2022. PMID: 35081326.
- [50] In practical execution on HPC machines, namely at the National Energy Research Scientific Computing Center using a Intel Xeon Processor E5-2698 v3 at 2.3 GHz, the difference in computational cost for using 96% and 92% compressed matrix amounts to  $\sim 77,000$  CPU-hrs. For the maximally compressed converged calculation (96% compression), the entire calculation amounts to  $\sim 60,000$  CPU-hrs.